The EMBO Journal vol.15 no.24 pp.6854–6862, 1996

Cloning, functional expression and brain localization of a novel unconventional outward rectifier K^+ channel

Michel Fink, Fabrice Duprat, Florian Lesage, Roberto Reyes, Georges Romey, Catherine Heurteaux and Michel Lazdunski[1]

Institut de Pharmacologie Moléculaire et Cellulaire, CNRS, 660, route des Lucioles, Sophia Antipolis, 06560 Valbonne, France

[1]Corresponding author

M.Fink and F.Duprat contributed equally to this work

Human TWIK-1, which has been cloned recently, is a new structural type of weak inward rectifier K^+ channel. Here we report the structural and functional properties of TREK-1, a mammalian TWIK-1-related K^+ channel. Despite a low amino acid identity between TWIK-1 and TREK-1 (~28%), both channel proteins share the same overall structural arrangement consisting of two pore-forming domains and four transmembrane segments (TMS). This structural similarity does not give rise to a functional analogy. K^+ currents generated by TWIK-1 are inwardly rectifying while K^+ currents generated by TREK-1 are outwardly rectifying. These channels have a conductance of 14 pS. TREK-1 currents are insensitive to pharmacological agents that block TWIK-1 activity such as quinine and quinidine. Extensive inhibitions of TREK-1 activity are observed after activation of protein kinases A and C. TREK-1 currents are sensitive to extracellular K^+ and Na^+. TREK-1 mRNA is expressed in most tissues and is particularly abundant in the lung and in the brain. Its localization in this latter tissue has been studied by *in situ* hybridization. TREK-1 expression is high in the olfactory bulb, hippocampus and cerebellum. These results provide the first evidence for the existence of a K^+ channel family with four TMS and two pore domains in the nervous system of mammals. They also show that different members in this structural family can have totally different functional properties.

Keywords: electrophysiology/heterologous expression/ *in situ* hybridization

Introduction

K^+ channels are ubiquitous membrane proteins that are involved in numerous cellular functions, in both excitable and non-excitable cells (Rudy, 1988; Hille, 1992). They are exceptionally diverse in their conductance, gating mechanism, pharmacology and molecular structure. The successful cloning and expression of a wide variety of pore-forming K^+ channel subunits in the past few years allowed the identification of different types of gene families. The first one is the *Shaker*-like family (Kv), corresponding to voltage-gated outward rectifier K^+ channel subunits with six transmembrane segments (TMS) (Betz, 1990; Pongs, 1992; Salkoff *et al.*, 1992; Jan and Jan, 1994). These channels have an important contribution in determining the frequency and duration of action potentials. They all possess a positively charged segment (S4) responsible for voltage sensitivity (Logothetis *et al.*, 1992; Bezanilla and Stefani, 1994). They are involved in neuronal integration, cardiac pace-making and hormone secretion. The second family is that of inward rectifying K^+ channels (Kir) which only have two TMS (Doupnik *et al.*, 1995). They play roles in the maintenance of resting potential and in the regulation of cell excitability. They have no S4 segment and inward rectification is due to intracellular block by polyamines or Mg^{2+} (Matsuda, 1991; Lu and Mackinnon, 1994; Nichols *et al.*, 1996). All pore-forming K^+ channel subunits cloned from *Drosophila*, vertebrates, yeasts and plants share a highly conserved sequence called the P domain that is part of the K^+-selective pore. This domain is considered as the signature of K^+ channels (Heginbotham *et al.*, 1994). The association of four pore-forming subunits is the minimal structure to create a K^+-selective pore (Pongs, 1993; Jan and Jan, 1994; Mackinnon, 1995).

New structural types of K^+ channels were isolated recently from yeast (Ketchum *et al.*, 1995; Zhou *et al.*, 1995; Lesage *et al.*, 1996a; Reid *et al.*, 1996) and human (Lesage *et al.*, 1996b). These channels contain two P domains. The number of TMS is eight for the yeast channel and four for the human channel called TWIK-1. Here we report the cloning and functional expression of a second member of the TWIK-1 K^+ channel structural family. Expressed in *Xenopus* oocyte, this new channel gives rise to a new type of outward rectifier K^+ current. Because of its overall structural similarity to TWIK-1, it was called TREK-1 (for TWIK-1 related K^+ channel). The localization of TREK-1 in the brain has been studied by *in situ* hybridization.

Results

Primary structure of TREK-1

The recent identification in human tissue of TWIK-1, a new structural and functional K^+ channel (Lesage *et al.*, 1996b), and the finding of at least five *Caenorhabditis elegans* genes encoding structural homologues (CeK putative K^+ channels) (Salkoff and Jegla, 1995; Lesage *et al.*, 1996b) strongly suggested the existence of related genes in mammals. In order to identify such genes, a cloning strategy employing degenerate PCR was developed. Alignment of TWIK-1 and related proteins from *C.elegans* revealed short conserved amino acid stretches, particularly in the second putative transmembrane domain M2 and the pore-forming region P2. Degenerate primers corresponding to both regions were designed and used to amplify a

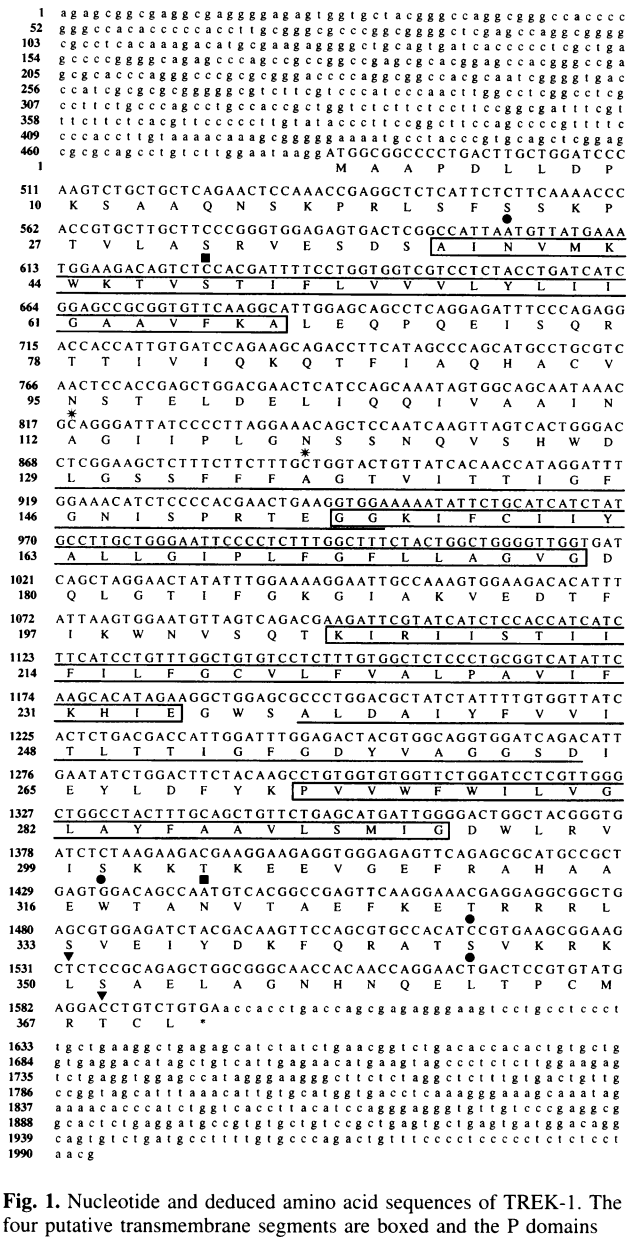

Fig. 1. Nucleotide and deduced amino acid sequences of TREK-1. The four putative transmembrane segments are boxed and the P domains are underlined. The transmembrane segments were deduced from a hydropathy profile computed with a window size of 11 amino acids according to Kyte and Doolitle (1982). Consensus sites for N-linked glycosylation (*) and phosphorylation by protein kinase C (●), protein kinase A (▼) or casein kinase II (■) are indicated. These sites have been identified using the prosite server (European Bioinformatics Institute) with the ppsearch software (EMBL Data library) based on the MacPattern program. The sequence of TREK-1 has been deposited in the GenBank/EMBL database under the accession No. U73488.

DNA fragment of ~280 bp with RT–PCR from mouse brain. Its sequencing revealed significant sequence similarities with the M2–P2 region of TWIK-1. This fragment was labelled and used to probe a mouse brain cDNA library under high stringency conditions. Four independent hybridizing clones were isolated. The sequence of the largest cDNA insert (~2.5 kb) contained an open reading frame (ORF) of 1113 bp. The deduced amino acid sequence corresponds to a 370 amino acid polypeptide with a calculated M_r of 40 791 (Figure 1). This protein contains two P domains (P1 and P2, Figure 1). Besides these domains, no significant alignment was observed between TREK-1 and other cloned K^+ channels except for TWIK-1 (see below). A comparative analysis of residues present in both P domains indicates a good conservation with the K^+-selective pore region of other cloned K^+ channels. In particular, one phenylalanine and two glycine residues are perfectly conserved (forming the canonical G–Y/F–G motif), as well as threonine and aromatic residues (tyrosine, tryptophan and phenylalanine) upstream of this conventional sequence (Heginbotham *et al.*, 1994). The hydrophobicity analysis of TREK-1 indicates the presence of four TMS, termed M1–M4 (Figure 1). Two potential N-linked glycosylation sites were found in the M1–P1 linker domain (residues 95 and 120) (Figure 1). There are also potential phosphorylation sites for protein kinase C (PKC) (residues 23, 300, 328 and 345), for protein kinase A (PKA) (residues 333 and 351) and for casein kinase II (residues 31 and 303) (Kemp and Pearson, 1990). Most of these potential phosphorylation sites (5/8) are located on the cytoplasmic C-terminus.

Alignment of TREK-1 and TWIK-1

The comparison of TWIK-1 and TREK-1 amino acid sequences is presented in Figure 2. This alignment clearly shows that both proteins share the same overall structure. The P1 domain is flanked by the hydrophobic M1 and M2 domains and P2 by M3 and M4 (Figure 2A and B). In both cases, an unusual loop (60 residues for TREK-1) is present between M1 and P1 that extends the length of the M1–P1 linker sequence thought to lie on the extracellular side of the membrane. TREK-1 is 34 amino acids longer than TWIK-1 because its NH_2- and COOH-termini are more extended. Despite a similar structural topology, the amino acid identity between TREK-1 and TWIK-1 is very low (~26%). Sequence homologies are not higher between TREK-1 and *C.elegans* sequences (25–28%) (not shown). The highest degree of sequence conservation between TREK-1 and TWIK-1 is in the two P domains and the M2 segment. In these regions, the amino acid identity reaches ~50% (Figure 2A). One intriguing feature of TWIK-1 is the presence of a non-conventional sequence in its P2 domain (G–L–G instead of G–Y/F–G). In TREK-1, both P1 and P2 domains are conventional and contain a GFG motif. This suggests that the two P domains are functional in TREK-1 and that the active TREK-1 K^+ channel is a dimeric association of TREK-1 subunits.

Tissue distribution and brain localization of TREK-1

The expression of TREK-1 mRNA in adult mouse tissues was examined by Northern blot analysis. As shown in Figure 3A, the TREK-1 probe detected a single transcript with an estimated size of ~3.8 kb. The level of TREK-1 expression is brain>lung>>kidney and heart>skeletal muscle (Figure 3A). No positive signal was obtained from the liver (not shown).

The localization of TREK-1 in the mouse brain was then studied by *in situ* hybridization. Low-power sagittal and coronal sections reveal that TREK-1 transcripts are widely expressed in the adult mouse brain (Figure 3B). Strongest signals are found in the olfactory bulb, hippocampal formation and cerebellum. The cerebral and piriform cortex show a moderate and homogeneous expression of TREK-1 mRNAs within neurons of all neocortical

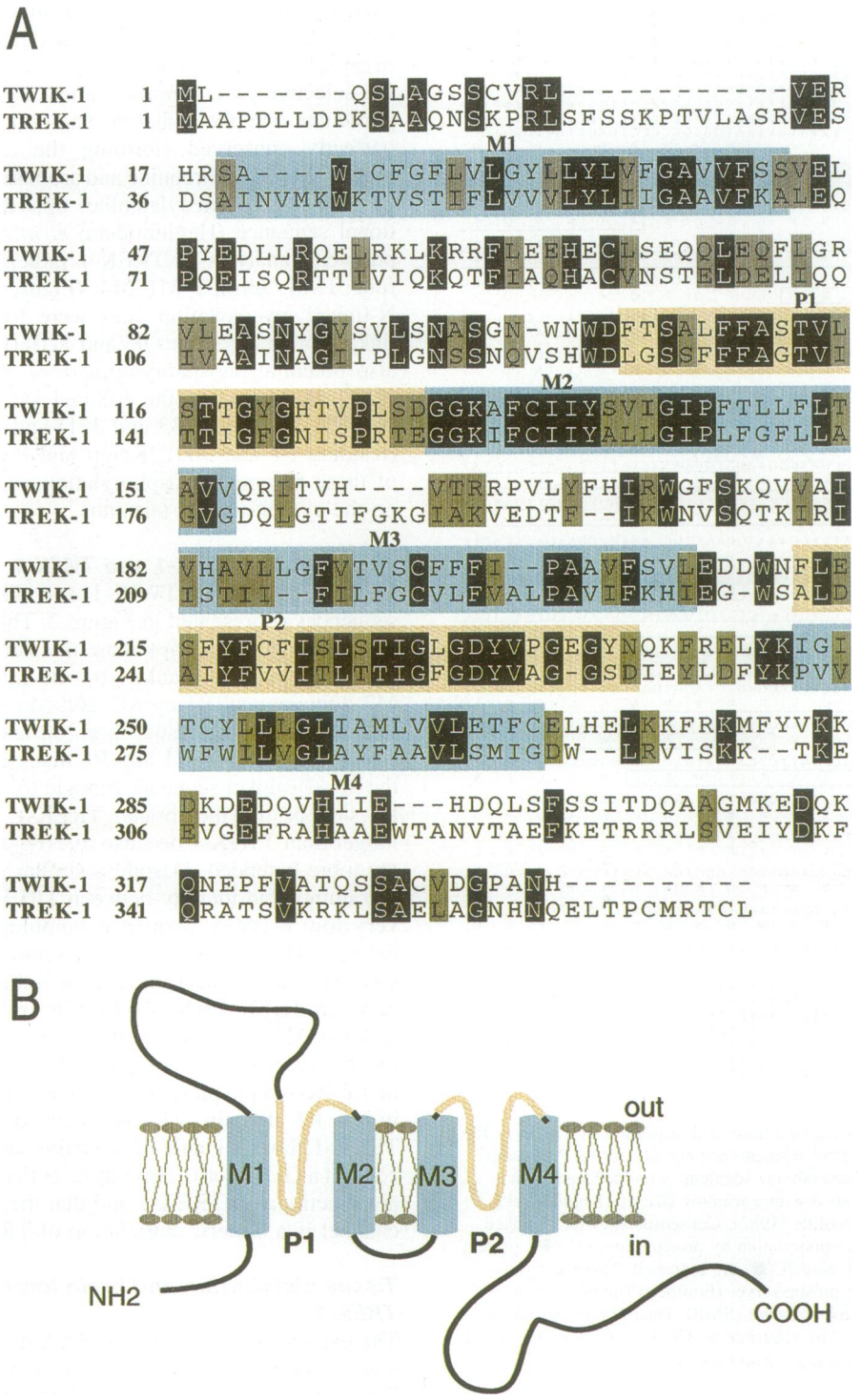

Fig. 2. Sequence comparison and structural model of TWIK-1 and TREK-1. (**A**) Alignment of TREK-1 and TWIK-1 amino acid sequences. Identical and conserved residues are boxed in black and grey, respectively. Dashes indicate gaps introduced for a better alignment. Relative positions of putative transmembrane segments (M1–M4) and P domains (P1 and P2) are also indicated. (**B**) Putative topology of TWIK-1 and TREK-1.

layers. Very low levels of expression were detected over most other regions including the hypothalamus, thalamic nuclei, habenula, substantia nigra, caudate putamen and globus pallidus of the basal ganglia, amygdaloid complex, midbrain and brain stem (pons and medulla). The expression of TREK-1 mRNA was examined further using dark-field photomicrographs of emulsion-dipped brain sections (data not shown). In the olfactory bulb, the glomeruli, the mitral cells and the internal granular layer showed the highest levels of TREK-1 transcripts as compared with the external plexiform layer. Periglomerular cells were highly labelled. In the hippocampal formation, the strongest labelling occurred over the granule cell bodies of the dentate gyrus, but substantial labelling was also

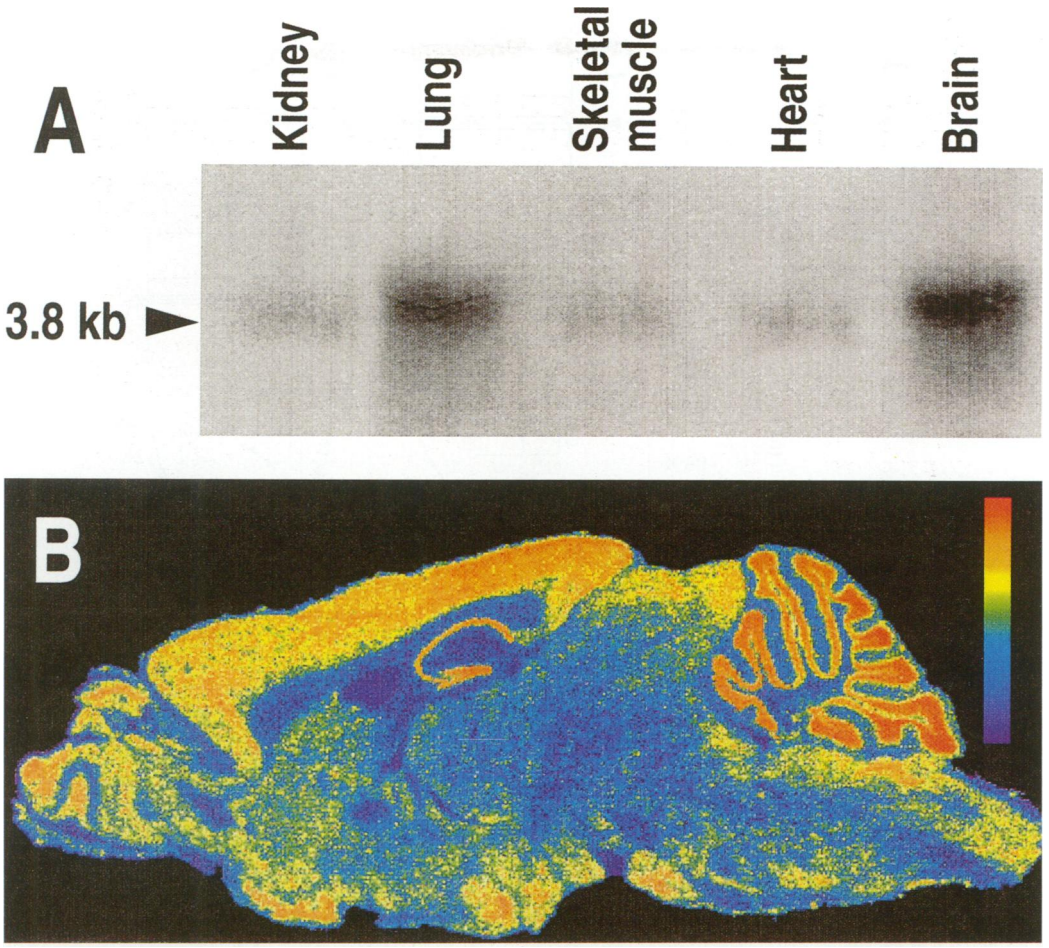

Fig. 3. Tissue and brain distribution of TREK-1 transcripts in mouse. (**A**) The expression of TREK-1 mRNAs was analysed by Northern blot in adult mouse tissues. Each lane represent 5 μg of poly(A)$^+$ RNAs. Autoradiographs were exposed for 48 h at −70°C. The size of messengers (kb) is indicated by an arrow. A control hybridization for comparison of levels in different tissues was carried out with a glyceraldehyde-3-phosphate dehydrogenase cDNA probe. (**B**) Digitized autoradiograph illustrating the distribution of TREK-1 mRNA in a parasagittal section of the mouse brain. Warmer colours represent higher levels of mRNA.

detected in all pyramidal cells in the CA1, CA2 and CA3 fields of Ammon's horn. A few neurons in the hilus of the dentate gyrus and in the molecular layer of Ammon's horn were also labelled. Remarkably high levels of TREK-1 transcripts were expressed in the granular layer of the cerebellar cortex. Cerebellar Purkinje cells and a few cells in the molecular layer, which may be stellate or basket cells, were positive. Weak signals were observed in the deep cerebellar nuclei.

Biophysical properties of TREK-1

For functional studies, the TREK-1 coding sequence was inserted between the 5′- and the 3′-untranslated sequences of *Xenopus* globin in the pEXO plasmid (Lingueglia *et al.*, 1993). Complementary RNA (cRNA) was transcribed from this construct and injected into *Xenopus laevis* oocytes. A non-inactivating current, not present in uninjected oocytes, was measured by two-electrode voltage-clamp (Figure 4A). Activation kinetics of the current are almost instantaneous and cannot be resolved from the capacitance discharge current recorded at the onset of the voltage pulse. The current–voltage relationship is outwardly rectifying, and almost no inward currents were recorded in the ND96 external medium containing 2 mM K^+ and 96 mM Na^+ (Figure 4A and B). When external Na^+ was substituted by K^+, the I–V curve was shifted rightward and downward. A decrease of the slope conductance between 0 and +50 mV, with 22.2 ± 3.7 μS in ND96 and 14.8 ± 3.3 μS (n = 4) in the K^+-rich solution (Figure 4B) and the activation of an inward current that was saturating upon hyperpolarization (Figure 4A and B) were observed. In order to elucidate this unusual behaviour, the separate effects of external K^+ and external Na^+ concentrations ([K^+]e and [Na^+]e) were studied. *N*-methyl D-glucamine (NMDG) was used to substitute these ions. Figure 4C shows the effect of external Na^+ on the TREK-1 currents. The currents are inhibited when Na^+ (96 mM) is substituted by NMDG (0 mM Na^+), with no variations of the currents recorded upon hyperpolarization. This inhibition is clearly voltage independent (Figure 4D). The current reversal potential is not affected significantly by the Na^+ concentration (−72 ± 5 mV and −62 ± 9 mV, n = 5, in 96 and 0 mM Na^+ respectively). The mean slope conductance between 0 and +50 mV is dose dependent and linear between 0 and 96 mM Na^+ with a slope of 140 nS/mM (Figure 4D, inset). It can be noted that this relationship at lower and higher [Na^+]e was not expected to be a linear function of [Na^+]e. The same

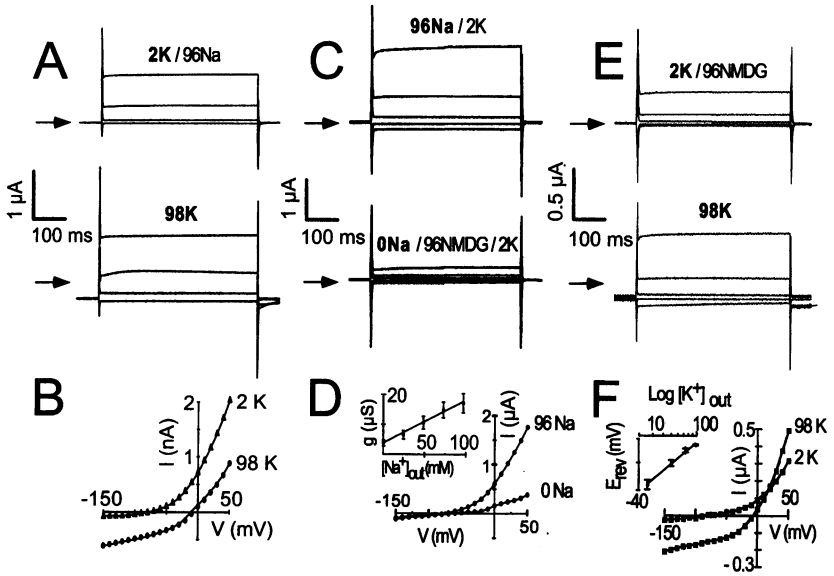

Fig. 4. Biophysical properties of TREK-1 currents expressed in *Xenopus* oocytes. (**A**) TREK-1 currents elicited by 500 ms voltage pulses to –100, –50, 0 and +50 mV from a holding potential of –80 mV, in ND96 external solution (2 mM K^+ and 96 mM Na^+) and in a K^+-rich solution (98 mM K^+). (**B**) Current–voltage relationship measured at the end of pulses as in (A), from –150 to +50 mV, in 10 mV steps, in ND96 and in 98 mM K^+. (**C**) TREK-1 currents elicited by 500 ms voltage pulses to –100, –50, 0 and +50 mV from a holding potential of –80 mV, in 2 mM K^+ and 0 or 96 mM external Na^+ (Na^+ is substituted by NMDG). (**D**) Current–voltage relationship measured at the end of pulses as in (C), from –150 to +50 mV, in 10 mV steps, in 96 mM Na^+ or in 0 mM Na^+ (96 mM NMDG). Inset: relationship between the mean slope conductance (measured between 0 and +50 mV) and external Na^+ concentration. (**E**) TREK-1 currents elicited by 500 ms voltage pulses to –100, –50, 0 and +50 mV from a holding potential of –80 mV in a modified ND96 solution containing 2 mM K^+ and 96 mM NMDG or 98 mM K^+. (**F**) Current–voltage relationship measured at the end of voltage pulses as in (E), from –150 to +50 mV in 10 mV steps, in low (2 mM K^+, 96 mM NMDG) or high (98 mM) K^+ solutions. Inset: reversal potentials of TREK-1 as a function of external K^+ concentrations (n = 4). In (A), (C) and (E), the zero current level is indicated by an arrow.

inhibition was observed when Na^+ was substituted by Li^+ instead of NMDG (data not shown), suggesting a specific effect of Na^+ ions on the activity of TREK-1 channels.

The effects of external K^+ have then been studied in an Na^+-free (96 mM NMDG) solution (Figure 4E, note the scale differences). Upon substitution of external NMDG by K^+, the reversal potential of the currents follows the K^+ equilibrium potential (E_K) (Figure 4F). A 10-fold change in external [K^+] leads to a 57.9 mV shift in the reversal potential values, in agreement with the Nernst equation (Figure 4F, inset), showing that TREK-1 is K^+ selective. In 98 mM external K^+, an inward current was revealed that saturated for negative potentials, and the outward current slope conductance between 0 and +50 mV was clearly enhanced from 3.8 ± 0.7 µS to 11.3 ± 4.3 µS (n = 5) in 2 and 98 mM K^+ respectively (Figure 4F).

We have shown previously that oocytes expressing TWIK-1 channels are more polarized that non-expressing oocytes, the resting membrane potential (E_m) reaching a value close to E_K (Lesage *et al.*, 1996b). The effect of TREK-1 on E_m was examined. In TREK-1-expressing oocytes, E_m was –81 ± 4 mV (n = 20, in standard ND96) instead of –43 ± 4 mV (n = 10) in non-injected oocytes (not shown). This result demonstrates that TREK-1, like TWIK-1, is able to drive E_m to a value close to E_K.

Pharmacology and regulation of TREK-1

The effect of various drugs on currents elicited by voltage pulses to +30 mV has been studied with the two-microelectrode method. The TREK-1 currents were insensitive to Cs^+ (100 µM), Gd^{3+} (100 µM), TEA (100 µM), quinine (100 µM), quinidine (100 µM), tedisamil (100 µM) and glibenclamide (10 µM). The K^+ channel opener P1060 (100 µM), a potent pinacidil analogue, was also without any effect. The only observed effect was obtained with Ba^{2+} that blocks 50% of TREK-1 currents at 100 µM (not shown). Other divalent cations such as Mg^{2+} were without effect.

TREK-1 currents were insensitive to intracellular acidification by CO_2 bubbling and to the variation of the intracellular Ca^{2+} obtained by injection of IP_3 (1 mM) or by application of the ionophore A23387 (10 µM). TREK-1 was also insensitive to the application of the permeant 8-Br-GMPc (300 µM). However, internal injection of GTPγS (100 µM) resulted in a decrease of TREK-1 currents by 42 ± 6% (n = 4), while injection of GDPβS produced a 38 ± 9% (n = 4) increase of activity (Figure 5A). These results suggest that TREK-1 currents are inhibited via a pathway involving G-protein activation. A direct effect of G-proteins on TREK-1 channels can probably be excluded since effects of nucleotides were maximal only after 5 min of application. Activation of G-proteins could lead to the activation of adenylate cyclase and/or phospholipase C, and the resulting increase of cAMP and/or diacylglycerol (DAG) levels could then lead to the activation of PKA and PKC, respectively. Then, the possible modulation of TREK-1 by activating PKA and PKC pathways was examined. Perfusion of a mixture of 3-isobutyl-1-methylxanthine (IBMX, 1 mM) and forskolin (10 µM) to increase intracellular cAMP levels resulted in 58 ± 6% (n = 5) inhibition of currents, while a perfusion of 40 nM of phorbol 12-myristate 13-acetate (PMA) to activate PKC resulted in a 45 ± 4% (n = 8) inhibition (Figure 5A). These two types of inhibition were

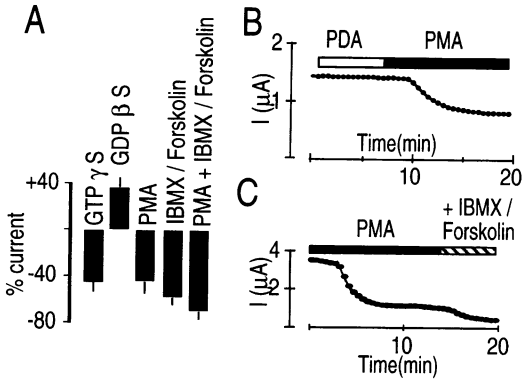

Fig. 5. Regulation of TREK-1 activity. (**A**) Bar graph showing the percentage of variations of peak currents elicited by voltage pulses to +50 mV after 10 min application of various drugs. GTPγS and GDPβS were intracellularly injected at a concentration of 100 μM. PMA (40 nM) and IBMX/forskolin mixture (1 mM and 10 μM, respectively) were added to the superfusate. (**B**) Effects of 40 nM PDA or PMA on currents obtained at +50 mV. (**C**) Additive effects of PMA and IBMX/forskolin on currents obtained at +50 mV.

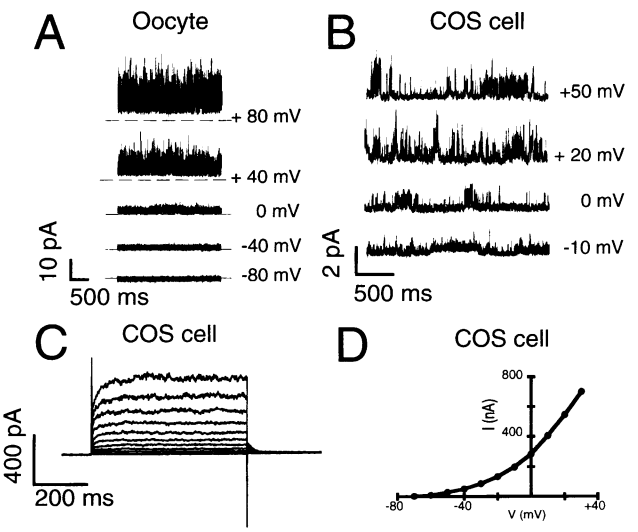

Fig. 6. Patch–clamp recording of TREK-1 currents expressed in oocytes and transfected COS cells. (**A**) TREK-1 current in inside-out recording at –80, –40, 0, +40 and +80 mV in oocytes. (**B**) TREK-1 current in inside-out recording at –10, 0, +20 and +50 mV in COS cells transiently transfected with TREK1. (**C**) COS whole-cell recordings of TREK-1 currents elicited by 500 ms voltage pulses from –80 to +30 mV, in 10 mV steps. (**D**) Current–voltage relationship recorded at the end of voltage pulses as in (C). In (C) and (D), the holding potential was –80 mV (close to E_K).

additive with a total decrease of 72 ± 5% of TREK-1 currents (Figure 5A and C). The application of the inactive PMA analogue, 4α-phorbol-12,13-didecanoate (PDA, 40 nM) was without effect (Figure 5B). These results suggest that TREK-1 activity is regulated via mechanisms implicating PKC as well as PKA.

Patch–clamp recordings of TREK-1 currents in oocytes and transfected COS cells

Inside-out patch recordings of TREK-1 currents in oocytes are displayed in Figure 6A. Upon depolarization, TREK-1 channels pass outward currents that are highly flickering. TREK-1 channels were also transiently expressed in COS cells. Figure 6C shows representative TREK-1 currents recorded from transfected cells. Untransfected or mock-transfected cells did not express any significant K^+ channels (not shown). As in the oocyte expression system, highly flickering outwardly rectifying currents were recorded in COS cells in the inside-out configuration (Figure 6B). The single channel conductance of these channels is 14 ± 2 pS (n = 5). Figure 6C shows whole-cell patch–clamp recordings in COS cells. TREK-1 currents expressed in oocytes and in COS cells are similar, with a slower rate of activation in COS cells (Figure 6C). TREK-1 currents in COS cells are clearly outwardly rectifying and their I–V relationship (Figure 6D) is very similar to the I–V curve obtained in oocytes. A substitution of external Na^+ by tetramethylammonium (TMA) produced a 63 ± 5% inhibition (n = 5) of the outward current at +50 mV (not shown).

Discussion

A new K^+ channel family in mammals

A novel mouse K^+ channel called TREK-1 has been cloned. It has four TMS and two P domains in its sequence. TREK-1 shares 28% amino acid identity and a conserved overall structure with the human TWIK-1 channel. Clearly, these two proteins belong to a new structural family of mammalian K^+ channels. The only related sequences that have been found to date are *C.elegans* genomic sequences deposited in DNA databases. These sequences called CeK (Salkoff and Jegla, 1995; Lesage *et al.*, 1996b) also probably correspond to functional K^+ channels in the nematode, but no expression of the CeK family of proteins has been obtained up till now. The isolation of TWIK-1 and TREK-1 channels in mammals establishes that the two P domain channel family is not restricted and specifically adapted to the nematode as was suggested earlier (Salkoff and Jegla, 1995).

The outward rectification of TREK-1 is unusual

Xenopus oocyte and COS cell expression studies revealed that TREK-1 channels pass much more outward currents upon depolarization than inward currents upon hyperpolarization. For this reason, they can be functionally classified as outward rectifier K^+ channels. However, the molecular mechanism of the outward rectification for TREK-1 and for 'classical' outward rectifier voltage-gated channels belonging to the *Shaker* superfamily (Kv) are clearly different. The Kv channels have six TMS and one of them, called S4, contains positive charges which are involved in the voltage sensing of these channels (Logothetis *et al.*, 1992; Bezanilla and Stefani, 1994). They are activated upon depolarization and opened from a fixed threshold potential whose value depends on the properties of their particular voltage sensor (S4). This threshold potential is always positive in relation to the K^+ equilibrium potential (E_K) and, in physiological conditions, Kv channels only pass outward currents. The TREK-1 structure does not present any domain similar to the positively charged S4 TMS which plays a crucial role in Kv channels. On the other hand, the TREK-1 threshold activation potential is not fixed, and closely follows the E_K. In light of these results, TREK-1 can be referred to as an 'unconventional' outward rectifier. The only channel which shares this unusual behaviour is the two P domain

yeast K^+ channel (Ketchum *et al.*, 1995; Zhou *et al.*, 1995; Lesage *et al.*, 1996a; Reid *et al.*, 1996). In the yeast channel, we have shown that the tendency of the channel preferentially to pass outward currents probably results from a mechanism intrinsic to the protein itself (Lesage *et al.*, 1996a). Occlusion of the inner mouth of the yeast channel pore by cations has been excluded (Lesage *et al.*, 1996a). Preliminary results with TREK-1 also seem to indicate that its rectification is due to an intrinsic mechanism, i.e. to structural elements contained in the protein sequence of the channel.

TWIK-1/TREK-1 structural homologies are not associated with functional similarities

Both the pharmacological and regulation properties of TREK-1 are very different from those previously described for TWIK-1. Unlike TWIK-1 (Lesage *et al.*, 1996a), TREK-1 is insensitive to quinine and quinidine. Unlike TWIK-1 (Lesage *et al.*, 1996a), TREK-1 is not inhibited by internal acidification and its activity is not enhanced by activation of PKC. In fact, the activity of TREK-1 channels is down-regulated by activation of PKC with phorbol esters and is also decreased drastically by phosphorylation processes involving PKA via indirect pathways that remain to be elucidated.

The most important difference between TREK-1 and TWIK-1 is of course in their rectification properties. TREK-1 has an outward rectification whereas TWIK-1 has an inward rectification. It is important to underline that a similar structural arrangement with four TMS and two P regions can give rise to completely different biophysical, pharmacological and regulation properties.

TREK-1 is found in very specific localizations in the brain

TWIK-1 and TREK-1 mRNAs are present in many mouse tissues. Both channels are expressed at the highest level in the brain. TREK-1 is particularly abundant in the olfactory bulb, hippocampal formation and cerebellum. The expression was moderate in the cerebral and piriform cortex, and very low in hypothalamus, thalamic nuclei, habenula, substantia nigra, caudate putamen and globus pallidus of the basal ganglia, amyloid complex, midbrain and brain stem.

What could be the biological significance of the $[K^+]e$ and $[Na^+]e$ dependence of TREK-1?

The almost time-independent gating of the TREK-1 channel as well as its capacity to drive E_m close to E_K suggests a physiological role as background K^+ conductance. An intriguing property of the TREK-1 channel is its activation by extracellular K^+ in a controlled external Na^+ concentration. This effect is unusual since an increase of $[K^+]e$ lowers the chemical driving force for outward K^+ flux and would be expected to decrease rather than increase TREK-1 outward currents. Nevertheless, such a $[K^+]e$ dependence has been reported for many heart and brain outward currents (Carmeliet, 1989; Pardo *et al.*, 1992; Sanguinetti and Jurkiewicz, 1992), and for cloned RCK4 (Kv1.4) and HERG K^+ channels (Pardo *et al.*, 1992; Sanguinetti *et al.*, 1995), and is well known for inward currents produced by inward rectifier K^+ channels (Sakmann and Trube, 1984). Kv1.4, a transient K^+ channel, has been shown to be sensitive to $[K^+]e$ and probably to underly $[K^+]e$-activated K^+ currents in hippocampal cells (Pardo *et al.*, 1992). It has been proposed that the $[K^+]e$ dependence of Kv1.4 has a role in the modulation of the firing frequency in neurons. In the case of cardiac HERG K^+ channels, the $[K^+]e$ dependence may modulate the duration of cardiac action potentials (Sanguinetti *et al.*, 1995). The effects of extracellular K^+ on the amplitude of TREK-1 outward current could be associated with the $[K^+]e$-induced variations in the neuronal excitability. On the other hand, this sensitivity to the external K^+ could have an importance in pathologies where large variations in $[K^+]e$ occur, such as epilepsy and brain or heart ischaemia (Heinemann, 1986; Gintant *et al.*, 1992).

In oocytes that express TREK-1, the increase of external K^+ gives rise to an inward current that saturates upon hyperpolarization. This phenomenon is potentially very interesting because the rise in external K^+ could make the K^+ equilibrium potential more positive than the resting potential and could then induce an inward K^+ current. Such a mechanism has long been proposed in glial cells for their role in the buffering of extracellular K^+ released from activated neurons (Ritchie, 1992). Though TREK-1 is not expressed in glial cells, such a regulatory role could be of importance in epithelial cells like pulmonary cells.

Finally, a particularly puzzling result is the sensitivity of TREK-1 to extracellular Na^+. Elevation of $[Na^+]e$ causes an increase in TREK-1 outward currents. Such an $[Na^+]e$-dependent activation has been described previously for an inward K^+ current recorded in the white bass retina (Pfeiffer-Linn *et al.*, 1995). The biological implications of this property are still mysterious for neuronal cells. This $[Na^+]e$ dependency may be an important consideration in lung and kidney where external Na^+ can vary significantly.

Materials and methods

Cloning of TREK-1 and RNA analysis

Two regions conserved between TWIK-1 and homologous products deduced from genes from *C.elegans* (Lesage *et al.*, 1996b) were determined by using standard alignment analysis. From the corresponding regions extending from Tyr137 to Pro143 (localized to the M2 segment) and from Thr225 to Tyr231 (localized to the P2 domain) of the TWIK-1 sequence, two degenerate primers were designed as follows: sense strand, 5′-GGAATTCTWYDSNBTNNTNRKNATHCC-3′; antisense strand, 5-CGGGATCCCWDRTCNCCNADNCCNAYNGT-3′ (conforming with the abbreviations recommended by the IUPAC-IUB), introducing *Eco*RI and *Bam*HI restriction sites for subcloning. Primers and adult mouse brain cDNAs were used for PCR amplification with the following profile: 94°C for 30 s, 45°C for 1 min, 72°C for 30 s, 38 cycles. Amplified products ranging from 100 to 500 bp were purified and used as template for a second round of PCR amplification under the same conditions. The PCR products of the expected size (250–300 bp) were digested with *Eco*RI and *Bam*HI then ligated into *Eco*RI–*Bam*HI-digested pBluescriptII SK^- (Stratagene). The 20 resulting plasmids were sequenced. One insert corresponded to a sequence related to TWIK-1. This fragment was ^{32}P labelled and used to screen a mouse brain cDNA library (Stratagene). Filters were hybridized in 50% formamide, 5× SSC, 4× Denhardt's solution, 0.1% SDS, 100 μg of denatured salmon sperm DNA at 50°C for 18 h and washed stepwise to a final stringency of 2× SSC, 0.3% SDS at 50°C. From 3×10^5 phages screened, four positives clones were obtained and excised from the λZAP XR vector into pBluescriptII SK^-. cDNA inserts were characterized by restriction analysis and by partial or complete sequencing on both strands by the dideoxy nucleotide chain termination method using an automatic sequencer (Applied Biosystems, model 373A). One clone (2.5 kb long) was shown to contain the full-length ORF and was designated pBS-TREK-1.

For Northern blot analysis, poly(A)$^+$ RNAs were isolated from mouse tissues and blotted onto nylon membranes as previously described (Lesage *et al.*, 1992). The blot was probed with the ^{32}P-labelled insert of pBS-TREK-1 in 50% formamide, 5× SSPE [0.9 M sodium chloride, 50 mM sodium phosphate (pH 7.4), 5 mM EDTA], 0.1% SDS, 5× Denhardt's solution, 20 mM potassium phosphate (pH 6.5) and 250 μg of denatured salmon sperm DNA at 50°C for 18 h and washed stepwise at 55°C to a final stringency of 0.2× SSC, 0.3% SDS.

In situ hybridization

Anaesthetized mice were perfused through the ascending aorta with 100 ml of 0.9% NaCl followed by 300 ml of ice-cold 4% paraformaldehyde (w/v) in 0.1 M sodium phosphate buffer (PBS, pH 7.4). The brains were dissected out, post-fixed for 2 h and immersed in a 20% sucrose–PBS solution. Sagittal and coronal frozen sections (12 μm) were mounted on poly-L-lysine-coated slides and stored at –70°C until use.

Two antisense synthetic oligonucleotides (49mer), complementary to the mouse cDNA sequence of TREK-1, corresponding to sequences from nucleotides 1 to 49 and 1065 to 1113 were used to detect TREK-1 transcripts. The sequences were the following: 5′-TGG AGT TCT GAG CAG CAG ACT TGG GAT CCA GCA AGT CAG GGG CCG CCA T-3′ and 5′-TCA CAG ACA GGT CCT CAT ACA CGG AGT CAG TTC CTG GTT GTG GTT GCC C-3′. Probes were 3′ end labelled with [α-^{33}P]dATP (3000 Ci/mmol, ICN Radiochemicals) by terminal deoxynucleotidyltransferase to an average specific activity of $1–2\times10^9$ d.p.m./μg. Sections were pre-hybridized for 1 h and hybridized overnight at 30°C with 4 pg of labelled probe in 35 μl of hybridization buffer containing 50% deionized formamide, 10% dextran sulphate, 500 mg/ml of denatured salmon sperm DNA, 1% Denhardt's, 5% Sarcosyl, 250 mg/ml yeast tRNA, 20 mM dithiothreitol, 20 mM $NaPO_4$ in 2× SSC. After hybridization, slides were washed in 1× SSC at 55°C twice for 30 min before dehydration, drying and apposition to Hyperfilm-βmax (Amersham) for 6 days. The specificity of hybridization was verified by control experiments in the presence of a 20-fold excess amount of the unlabelled oligonucleotide and with sense probes.

Electrophysiological measurements in Xenopus oocytes

The entire coding sequence of TREK-1 was amplified by PCR using a low error rate DNA polymerase (Pwo DNA polymerase, Boehringer) and subcloned into the pEXO vector (Lingueglia *et al.*, 1993) to give pEXO-TREK-1. Capped cRNAs were synthesized *in vitro* from the linearized plasmid by using the T7 RNA polymerase (Stratagene). *Xenopus laevis* were purchased from CRBM (Montpellier, France). Preparation and cRNA injection of oocytes has been described elsewhere (Guillemare *et al.*, 1992). Oocytes were used for electrophysiological studies 2–4 days following injection. In a 0.3 ml perfusion chamber, a single oocyte was impaled with two standard microelectrodes (1–2.5 MΩ resistance) filled with 3 M KCl and maintained under voltage clamp by using a Dagan TEV 200 amplifier. Stimulation of the preparation, data acquisition and analysis were performed using pClamp software (Axon instruments, USA). Drugs were applied externally by addition to the superfusate (flow rate 3 ml/min) or intracellularly injected by using a pressure microinjector (Inject+Matic, Switzerland). All experiments were performed at room temperature (21–22°C). For patch–clamp experiments, devitellinized oocyte inside-out patches were perfused with a solution containing 150 mM KCl, 3 mM $MgCl_2$, 5 mM EGTA, and 10 mM HEPES at pH 7.2 with KOH. Pipettes were filled with the standard ND96 solution supplemented with 100 μM $GdCl_3$ to inhibit the activity of endogenous stretch-activated channels.

Patch–clamp recordings in transfected COS cells

For expression in COS cells, the coding sequence of TREK-1 was subcloned into the pCi plasmid (Promega) under the control of the cytomegalovirus promoter to give pCi-TREK-1. COS cells were seeded at a density of 70 000 cells per 35 mm dish 24 h prior transfection. Cells were then transfected by the classical calcium phosphate precipitation method with 2 μg of pCI-TREK-1 and 1 μg of CD8 plasmids. Transfected cells were visualized 48 h after transfection using the anti-CD8 antiboby-coated beads method (Jurman *et al.*, 1994). For electrophysiological recordings, the internal solution contained 150 mM KCl, 3 mM $MgCl_2$, 5 mM EGTA, and 10 mM HEPES at pH 7.2 with KOH, and the external solution 150 mM NaCl, 5 mM KCl, 3 mM $MgCl_2$, 10 mM HEPES at pH 7.4 with NaOH.

Acknowledgements

We are very grateful to N.Leroudier, G.Jarretou, M.Jodar and N.Gomez for expert technical assistance, to D.Doume for secretarial assistance, and to F.Aguila for artwork. F.L. was the recipient of a grant from the Fondation pour la Recherche Médicale. This work was supported by the Association contre les Myopathies (AFM), the Centre National de la Recherche Scientifique (CNRS); thanks are due to Bristol Myers Squibb Company for an 'Unrestricted Award'.

References

Betz,H. (1990) Homology and analogy in transmembrane channel design: lessons from synaptic membrane proteins. *Biochemistry*, **29**, 3591–3599.

Bezanilla,F. and Stefani,E. (1994) Voltage-dependent gating of ionic channels. *Annu. Rev. Biophys. Struct.*, **23**, 819–846.

Carmeliet,E. (1989) K^+ channels in cardiac cells: mechanisms of activation, inactivation, rectification and K^+e sensitivity. *Pflugers Arch.*, **414**, S88–S92.

Doupnik,C.A., Davidson,N. and Lester,H.A. (1995) The inward rectifier potassium channel family. *Curr. Opin. Neurobiol.*, **5**, 268–277.

Gintant,G.A., Cohen,I.S., Datyner,N.B. and Kline,R.P. (1992) Time-dependent outward currents in the heart. In Fozzard,H.A., Jennings,R.B., Haber,E., Katz,E.M. and Morgan,H.E. (eds), *The Heart and Cardiovascular System*. Raven Press, New York, pp. 1121–1169.

Guillemare,E., Honore,E., Pradier,L., Lesage,F., Schweitz,H., Attali,B., Barhanin,J. and Lazdunski,M. (1992) Effects of the level of messenger RNA expression on biophysical properties, sensitivity to neurotoxins, and regulation of the brain delayed-rectifier K^+ channel Kv1.2. *Biochemistry*, **31**, 12463–12468.

Heginbotham,L., Lu,Z., Abramson,T. and Mackinnon,R. (1994) Mutations in the K^+ channel signature sequence. *Biophys. J.*, **66**, 1061–1067.

Heinemann,U. (1986) Excitatory amino acids and epilepsy-induced changes in extracellular space size. *Adv. Exp. Med. Biol.*, **203**, 449–460.

Hille,B. (1992) *Ionic Channels of Excitable Membranes*. 2nd edn. Sinauer Associates Inc., Sunderland, MA.

Jan,L.Y. and Jan,Y.N. (1994) Potassium channels and their evolving gates. *Nature*, **371**, 119–122.

Jurman,M.E., Boland,L.M. and Yellen,G. (1994) Visual identification of individual transfected cells for electrophysiology using antibody-coated beads. *BioTechniques*, **17**, 876–881.

Kemp,B.E. and Pearson,R.B. (1990) Protein kinase recognition sequence motifs. *Trends Biochem. Sci.*, **15**, 342–346.

Ketchum,K.A., Joiner,W.J., Sellers,A.J., Kaczmarek,L.K. and Goldstein, S.A.N. (1995) A new family of outwardly rectifying potassium channel proteins with two pore domains in tandem. *Nature*, **376**, 690–695.

Kyte,J. and Doolittle,R. (1982) A simple model for displaying the hydropathic character of a protein. *J. Mol. Biol.*, **157**, 105–106.

Lesage,F., Attali,B., Lazdunski,M. and Barhanin,J. (1992) Developmental expression of voltage-sensitive K^+ channels in mouse skeletal muscle and C2C12 cells. *FEBS Lett.*, **310**, 162–166.

Lesage,F., Guillemare,E., Fink,M., Duprat,F., Lazdunski,M., Romey,G. and Barhanin,J. (1996a) A pH-sensitive yeast outward rectifier K^+ channel with two pore domains and novel gating properties. *J. Biol. Chem.*, **271**, 4183–4187.

Lesage,F., Guillemare,E., Fink,M., Duprat,F., Lazdunski,M., Romey,G. and Barhanin,J. (1996b) TWIK-1, a ubiquitous human weakly inward rectifying K^+ channel with a novel structure. *EMBO J.*, **15**, 1004–1011.

Lingueglia,E., Voilley,N., Waldmann,R., Lazdunski,M. and Barbry,P. (1993) Expression cloning of an epithelial amiloride-sensitive Na^+ channel—a new channel type with homologies to *Caenorhabditis elegans* degenerins. *FEBS Lett.*, **318**, 95–99.

Logothetis,D.E., Movahedi,S., Satler,C., Lindpaintner,K. and Nadalginard,B. (1992) Incremental reductions of positive charge within the S4 region of a voltage-gated K^+ channel result in corresponding decreases in gating charge. *Neuron*, **8**, 531–540.

Lu,Z. and Mackinnon,R. (1994) Electrostatic tuning of Mg^{2+} affinity in an inward-rectifier K^+ channel. *Nature*, **371**, 243–246.

Mackinnon,R. (1995) Pore loops: an emerging theme in ion channel structure. *Neuron*, **14**, 889–892.

Matsuda,H. (1991) Magnesium gating of the inwardly rectifying K^+ channel. *Annu. Rev. Physiol.*, **53**, 289–298.

Nichols,C.G., Makhina,E.N., Pearson,W.L., Sha,Q. and Lopatin,A.N. (1996) Inward rectification and implications for cardiac excitability. *Circ. Res.*, **78**, 1–7.

Pardo,L.A., Heinemann,S.H., Terlau,H., Ludewig,U., Lorra,C., Pongs,O. and Stühmer,W. (1992) Extracellular K^+ specifically modulates a rat brain potassium channel. *Proc. Natl Acad. Sci. USA*, **89**, 2466–2470.

Pfeiffer-Linn,C., Perlman,I. and Lasater,E.M. (1995) Sodium dependency of the inward potassium rectifier in horizontal cells isolated from the white bass retina. *Brain Res.*, **701**, 81–88.

Pongs,O. (1992) Molecular biology of voltage-dependent potassium channels. *Physiol. Rev.*, **72**, S69–S88.

Pongs,O. (1993) Structure–function studies on the pore of potassium channels. *J. Membr. Biol.*, **136**, 1–8.

Reid,J.D., Lukas,W., Shafaatian,R., Bertl,A., Scheurmannkettner,C., Guy,H.R. and North,R.A. (1996) The *S.cerevisiae* outwardly-rectifying potassium channel (DUK1) identifies a new family of channels with duplicated pore domains. *Receptors and Channels*, **4**, 51–62.

Ritchie,J.M. (1992) Voltage-gated ion channels in Schwann cells and glia. *Trends Neurosci.*, **15**, 345–351.

Rudy,B. (1988) Diversity and ubiquity of K^+ channels. *Neuroscience*, **25**, 729–749.

Sakmann,B. and Trube,G. (1984) Conductance properties of single inwardly rectifying potassium channels in ventricular cells from guinea pig heart. *J. Physiol.*, **347**, 641–657.

Salkoff,L. and Jegla,T. (1995) Surfing the DNA databases for K^+ channels nets yet more diversity. *Neuron*, **15**, 489–492.

Salkoff,L., Baker,K., Butler,A., Covarrubias,M., Pak,M.D. and Wei,A.G. (1992) An essential set of K^+ channels conserved in flies, mice and humans. *Trends Neurosci.*, **15**, 161–166.

Sanguinetti,M.C. and Jurkiewicz,N.K. (1992) Role of external Ca^{2+} and K^+ in gating of cardiac delayed rectifier K^+ currents. *Pflügers Arch.*, **420**, 180–186.

Sanguinetti,M.C., Jiang,C.G., Curran,M.E. and Keating,M.T. (1995) A mechanistic link between an inherited and an acquired cardiac arrhythmia: HERG encodes the I-Kr potassium channel. *Cell*, **81**, 299–307.

Zhou,X.L., Vaillant,B., Loukin,S.H., Kung,C. and Saimi,Y. (1995) YKC1 encodes the depolarization-activated K^+ channel in the plasma membrane of yeast. *FEBS Lett.*, **373**, 170–176.

Received on August 20, 1996; revised on October 2, 1996